REPUBLIC OF AZERBAIJAN

On the rights of the manuscript

PREPARATION AND INVESTIGATION OF NEW COMPOSITES BASED ON BUTADIENE RUBBER FOR IMMOBILIZATION OF ZnS NANOPARTICLES

ABSTRACT

of the dissertation for the degree of Doctor of Philosophy

Specialty: 2317.01 - Nanochemistry and nanomaterials

Field of science: Chemistry

Applicant: **Nada Edres Mohammed Abdala**

Baku – 2025

The work was performed at the Department of High Molecular Compounds Chemistry of the Baku State University.

Scientific supervisor: Doctor of Chemical Sciences, professor **Rasim Mirali Alosmanov**

Official opponents: Corresponding member of ANAS, doctor of chemical sciences, professor **Islam Israfil Mustafayev,**

Full member of ANAS, doctor of chemical sciences, professor **Adil Abdulkhalig Garibov,**

Corresponding member of ANAS, doctor of chemical sciences, professor **Eldar Bahadir Zeynalov**

Dissertation council BED 2.16 of Supreme Attestation Commission under the President of the Republic of Azerbaijan operating at Baku State University

Chairman of the Dissertation council — doctor of chemical sciences, professor **Ibrahim Garib Mammadov**

Scientific secretary of the Dissertation council — doctor of chemical sciences, dosent **Farid Nadir Naghiyev**

Chairman of the scientific seminar — Full member of ANAS, doctor of chemical sciences, professor **Vagif Majid Farzaliyev**

Azərbaycan Respublikasının Elm və Təhsil Nazirliyi
BAKI DÖVLƏT UNİVERSİTETİ p.h.ş.
Ministry of Science and Education of the Republic of Azerbaijan
Baku State University (j.s.c.)
ELMİ KATİB
SCIENTIFIC SECRETARY
İmzanı təsdiq edirəm:
"10" 07 2025

GENERAL CHARACTERISTICS OF THE WORK

The topic's degree of development and its actuality. Nanocomposites are considered to be among the most advanced and newest representatives of 21st-century hybrid materials. These composites consist of at least two phases, one of which is nanoscale. Due to their unique properties and potential applications, they are considered promising for various industries. Depending on the type of matrix used, nanocomposites can be divided into three main categories: metal matrix nanocomposites, ceramic matrix nanocomposites and polymer matrix nanocomposites (PNCs).

PNCs are composites consisting of nanoparticles dispersed in a polymer matrix[1]. They have a wide range of industrial applications due to their lightness, low cost and variety of properties. Numerous polymers perform different functions in nanocomposites, such as stabilisers, coating agents and nanoreactors. Taking the above into account, polymers are considered to be the most suitable material for preparing nanocomposites with novel optical and electrical properties[2].

In recent years, PNCs synthesised using various methods and containing different types of nanoparticles (metals, oxides and sulphides) have been used effectively as sensors, solar cell components, catalysts and membranes. However, the synthesis of PNCs has certain disadvantages. For example, different molecular structure of the polymer matrix, specific conditions selected for each synthesis and etc. Various approaches have been proposed to overcome the disadvantages, one of which involves preparing

---

[1] Ramakoti, I.S. A brief review on polymer nanocomposites: current trends and prospects / I.S. Ramakoti, A.K. Panda, N. Gouda // Journal of Polymer Engineering, - 2023. 43 (8), - p. 651-679. https://doi.org/10.1515/polyeng-2023-0103.

[2] Peng, S.L., Chen, G.Y., Hsu, S.W. Tuning the Optical and Electrical Properties of Polymer-Based Nanocomposites by Plasmon-Induced Electromagnetic Field. Advanced materıals ınterfaces, 2022, 9 (15), 2200089. https://doi.org/10.1002/admi.202200089.

PNCs with the directed immobilisation of nanoparticles. The functionality of polymers and the presence of fillers with different structures in the matrix are also important factors in the immobilisation of nanoparticles. Therefore, the development and preparation of new matrices consisting of functional polymers and polymer/filler systems for the immobilisation of nanoparticles is the focus of this thesis.

Object and subject of the research. Butadiene rubber (BR), expanded perlite (EP), modified expanded perlite (PhEP) and carbon black (CB) of P-234 grade and ZnS nanoparticles are chosen as objects of research. The subject of the study is to obtain composites based on the listed polymers and fillers, to study their structural properties, thermal and electrical properties. In addition, the composites were used for immobilisation of ZnS nanoparticles, and the electrical, antibacterial and photocatalytic properties of the obtained PNC were investigated in detail.

Aims and objectives of the research. The aim of the work is to carry out the oxidative chlorophosphorylation (OxCh) reaction of BR with the participation of EP, PhEP, CB, to obtain three- dimensional spatially networked polymer/filler composites (PhBR, EP/PhBR, PhEP/PhBR and CB/PhBR) with the subsequent hydrolysis of the intermediate product, to determine the structural properties of the composites, as well as their thermal and electrical properties depending on the nature of the filler. Immobilisation of ZnS nanoparticles into various BR-based matrices using the SILAR method, investigation of the structure of nanocomposites as well as their antimicrobial/photocatalytic activity are also among the aims and objectives of the thesis work.

Research methods. The synthesis of the PhBR, EP/PhBR, PhEP/PhBR and CB/PhBR composites was achieved using an OxF reaction followed by hydrolysis of the reaction products. The SILAR method was used to immobilise ZnS nanoparticles. The structural, electrical and thermal stability properties, as well as the antibacterial and photocatalytic activity, of the samples were studied using the following methods: Fourier transform infrared spectroscopy (FTIR), ultraviolet–visible spectroscopy (UV-vis),

X-ray phase analysis (XRD), scanning electron microscopy (SEM), thermogravimetry (TG) and the Coats–Redfern method (for thermal decomposition kinetics). The Brunauer–Emmett– Teller (BET) method was used to determine capacitance on an LTSR E7-20 at angular frequencies ranging from 1 kHz to 1000 kHz. The disc diffusion method was used to test the samples' activity against Gram-positive (+G) and Gram-negative (-G) bacteria. The photocatalytic activity of the samples was studied using the decomposition of crystal violet (CV) dye under visible light as an example.

Conceptual issues presented for defence:

1. Functionalisation of EP using the OxCh reaction
2. Synthesis of new composites based on BR, EP, PhEP, CB using OxCh reaction
3. Analysis of the structures of BR, EP/PhBR, PhEP/PhBR, CB/PhBR composites, investigation of their electrical, dielectric and thermal properties;
4. Synthesis of new nanocomposites (ZnS/PhBR, ZnS/EP- PhBR, ZnS/PhEP-PhBR and ZnS/CB-PhBR) via the SILAR method.
5. Study of structural features and electrical properties of ZnS/PhBR, ZnS/EP-PhBR, ZnS/PhEP-PhBR, ZnS/CB-PhBR nanocomposites;
6. Comparison of the antimicrobial activity of ZnS/PhBR, ZnS/EP-PhBK, ZnS/PhEP-PhBR, ZnS/CB-PhBR nanocomposites with the corresponding properties of "pure" ZnS nanoparticles;
7. Comparison of the photocatalytic activity of ZnS/PhBR, ZnS/EP-PhBR, ZnS/PhEP-PhBR, ZnS/CB-PhBR nanocomposites with the corresponding properties of "pure" ZnS nanoparticles.

The scientific novelty of the research.

1. For the first time, EP was functionalised using the OxCh reaction to create a chemical affinity between BR and EP.
2. To obtain new types of BR-based composites, the joint OxCh reaction of EP, PhEP and CB with a polymer was carried out.

3. The structure of the prepared BR-based composites (PhBR, EP/PhBR, PhEP/PhBR and CB/PhBR) was confirmed by various research methods. The ion-exchange capacity and thermal and electrical properties were also determined
4. New nanocomposites (ZnS/PhBR, ZnS/EP-PhBR, ZnS/PhEP-PhBR and ZnS/CB-PhBR) were prepared using the SILAR method.
5. The structure of the ZnS/PhBR, ZnS/EP-PhBR, ZnS/PhEP-PhBR and ZnS/CB-PhBR nanocomposites was studied.
6. The antimicrobial and photocatalytic activity of the nanocomposites have been analysed.

Theoretical and practical significance of the research study:

1. The ideas and approaches proposed in the dissertation are important for developing and preparing new types of composites for the immobilisation and stabilisation of nanoparticles, using cheap, environmentally friendly and easily available reagents and materials. Nanocomposites prepared using this approach offer new opportunities for industrial technology.
2. The prepared composites (PhBR, EP/PhBR, PhEP/PhBR and CB/PhBR) are an interesting matrix for the immobilisation of ZnS nanoparticles, thereby increasing their lifetime.
3. New nanocomposites will enable ZnS to be used in sensors, energy harvesters, hydrogen generation and other applications.
4. The new composites can also be applied for immobilization of other nanoparticles.
5. In addition to stabilising nanoparticles, new composites can be used as adsorbents and refractory materials.

Validation and application. 5 scientific articles and 11 theses of reports have been published on the subject of the thesis. 4 articles were published in journals indexed in Web of Science (Science Citation Index Expanded), 1 - in international scientific databases Scopus.

The dissertation work was approved at international and republican scientific conferences: V International (XV Ukrainian)

Conference, Vinnytsia- Ukraine, 2022; IV International Conference on Ankara Scientific Research, Ankara, Turkey, 2022; ASES International Conference on Health, Engineering and Science, Ankara, Turkey, 2002; Modern Problems of Theoretical and Experimental Chemistry, International Scientific Conference, Baku, 2022; Republican Scientific Conference of Doctoral Students, Master's Students and Young Researchers "Chemistry and Chemical Technology" dedicated to the 99th anniversary of the birth of the National Leader Heydar Aliyev, Baku, 2022; International Scientific and Practical Conference "Fundamental and Practical Aspects of Functional Polymers", Tashkent, 2023; 7th International Congress of Innovative and Modern Scientific Research, Tokyo, 2023; Republican Scientific Conference of Doctoral Students, Master's Students and Young Researchers "Chemistry and Chemical Technology" dedicated to the 100th anniversary of the birth of the National Leader Heydar Aliyev, Baku, 2023; 8th International Conference on Modern Trends in Physics, Baku, 2023; 22nd Mendeleev Congress on General and Applied Chemistry, Moscow.

Name of the organisation where the dissertation work was complited. The research work within the scope of the dissertation topic was carried out at the Department of High Molecular Compounds Chemistry, Faculty of Chemistry, Baku State University.

The structure and scope of the dissertation. The dissertation consists of an introduction (19,934 characters), five chapters (147,092 characters) including a summary of experimental and analysis results, a conclusion, and a bibliography of 292 sources. The dissertation was written in total of 194 pages, including 20 tables, 12 schemes, and 43 Figures.

Personal contribution of the author. The doctorant collected and analysed literature data, pre-modified the EP, prepared composites and immobilised ZnS nanoparticles. The author played a key role in studying the prepared samples, interpretation of the results obtained, and preparing scientific publications.

MAIN CONTENT OF THE WORK

The introduction presents the relevance of the dissertation topic, its purpose, scientific novelty and the methodology of practical processes used for synthesis, as well as the approval of the obtained results.

The first chapter provides a review of the literature based on recent research on nanomaterials and nanocomposites. The synthesis, structural properties and study of matrices used in the preparation of PNC are described in sufficient detail. Special attention is paid in this chapter to information dedicated to the synthesis and application of PNC with ZnS particles.

The second chapter presents the methods, materials, reagents and reaction procedures used for the synthesis of samples in the dissertation work, instrumental analysis methods used in the study of the structure and properties of the prepared nanocomposites.

The first part of the **third chapter** is devoted to the transformation of EP by the OxCh reaction, the synthesis of the sample by hydrolysis of the transformation product, its analysis using the FTIR, UV-vis, XRD, SEM and BET methods, as well as the study of the thermal and electrical properties of PhEP.

EP modification was carried out by the OxCh reaction in the presence of oxygen with PCl_3 (the reaction is exothermic), followed by hydrolysis of the obtained sample. It should be noted that the OxCh reaction is also exothermic for organic compounds and polymers.

The structures of EP and its modified forms were studied using the FTIR spectroscopy method (Fig. 1). The peaks at 1000 cm^{-1}, 3650-3350 cm^{-1}, 787 cm^{-1} and 1628 cm^{-1} absorption bands in the spectrum of the original EP are associated with Si-O, Si-OH, Si-O-Al and adsorbed water molecules. Comparatively, a similar spectrum was recorded in the PhEP sample with some differences: the shoulder appearing at 787-758 cm^{-1} and 1083-1000 cm^{-1} is associated with a certain overlap of the absorption bands of P=O, P-OH groups, and modified silanol groups (Si-OH).

In addition, the absorption band at 3100-3600 cm-1 in PhEP is broader. This can be explained by the presence of -P(O)(OH)$_2$ groups. The low intensity of the peaks in the spectrum of PhEP indicates that the Si-O-Si fragment is partially broken as a result of the modification of the surface of EP by -P(O)(OH)$_2$ groups.

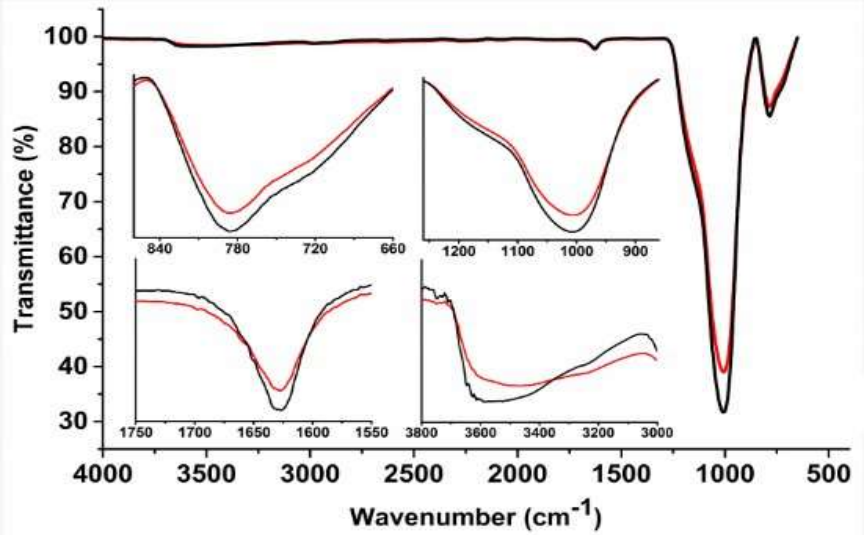

Fig. 1. FTIR spectra of EP (black) and PhEP (red)

In the UV-vis spectrum of EP (Fig. 2), a broad peak at 243 nm confirms the presence of silicon, which is the main component. This is a characteristic signal of aluminosilicates. In PhEP, a characteristic peak appears at 254 nm. The shift of the peak to a lower wavelength range is due to a quantum size change in the structure, which indicates the presence of -P(O)(OH)$_2$ groups in the sample.

The decrease in the width of the forbidden band of EP (Fig. 3) calculated (directly and indirectly) by the Tauc equation indicates the effect of -P(O)(OH)$_2$ groups on the microscopic structure of EP.

$$(\alpha h\nu)^n = C(h\nu - E_g)$$

where h is Planck's constant; C is a constant; ν is the frequency; Eg is the forbidden optical band gap; α is the absorption coefficient; and n is 1/2 for indirectly allowed transitions and 2 for directly allowed transitions.

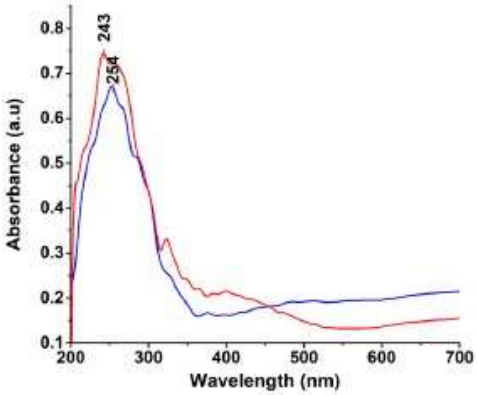

Fig. 2. UV-visible spectra of EP (blue) and PhEP(red)

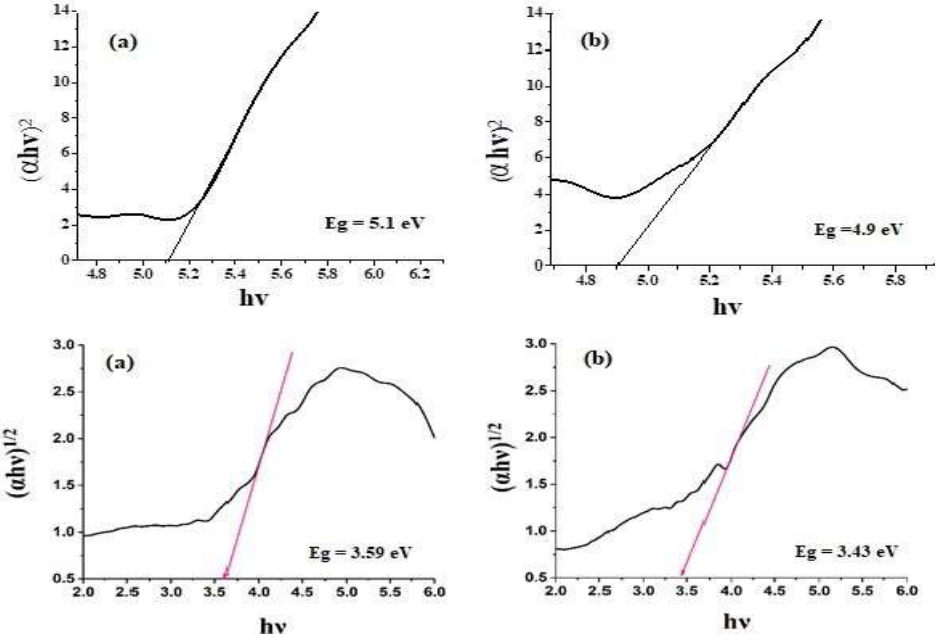

Fig. 3. Direct and indirect optical band gap calculation of EP (a,a) and PhEP (b,b)

The broad peak from 10° 2θ to 40° 2θ in the diffractogram of EP (Fig. 4) indicates the amorphous nature of EP.

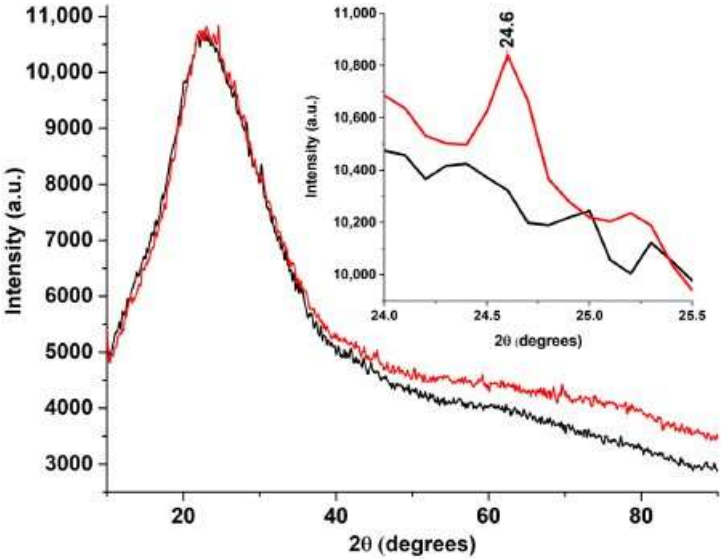

Fig. 4. XRD spectra of EP (black) and PhEP (red)

A similar peak is also observed in the sample obtained after modification by the OxCh reaction. This indicates that no changes occur in the structure of EP as a result of the modification and that modification with -$P(O)(OH)_2$ groups occurs only on the surface. A small peak is observed in the diffractogram of PhEP at 24.6° 2θ, indicating an increase in the amount of SiO_2. It is known that EP contains various oxides (Al_2O_3, CaO, MgO, Fe_2O_3, Na_2O and K_2O), which can react with the acid formed during the reaction and be washed out of the main mass (EP) during the hydrolysis process. Therefore, the peak corresponding to SiO_2 (which does not interact with the acid) appears more intense.

In the SEM image, it is observed that EP has a regular layered structure (Fig. 5a), while in the PhEP sample the surface is smoother, which is also a result of the modification (Fig. 5b). Compared to the elemental analysis of EP (according to the results of energy- dispersive X-ray analysis), 14% phosphorus is visible in PhEP and the amount of oxygen is also increased. This result confirms the presence of -$P(O)(OH)_2$ groups in the PhEP sample.

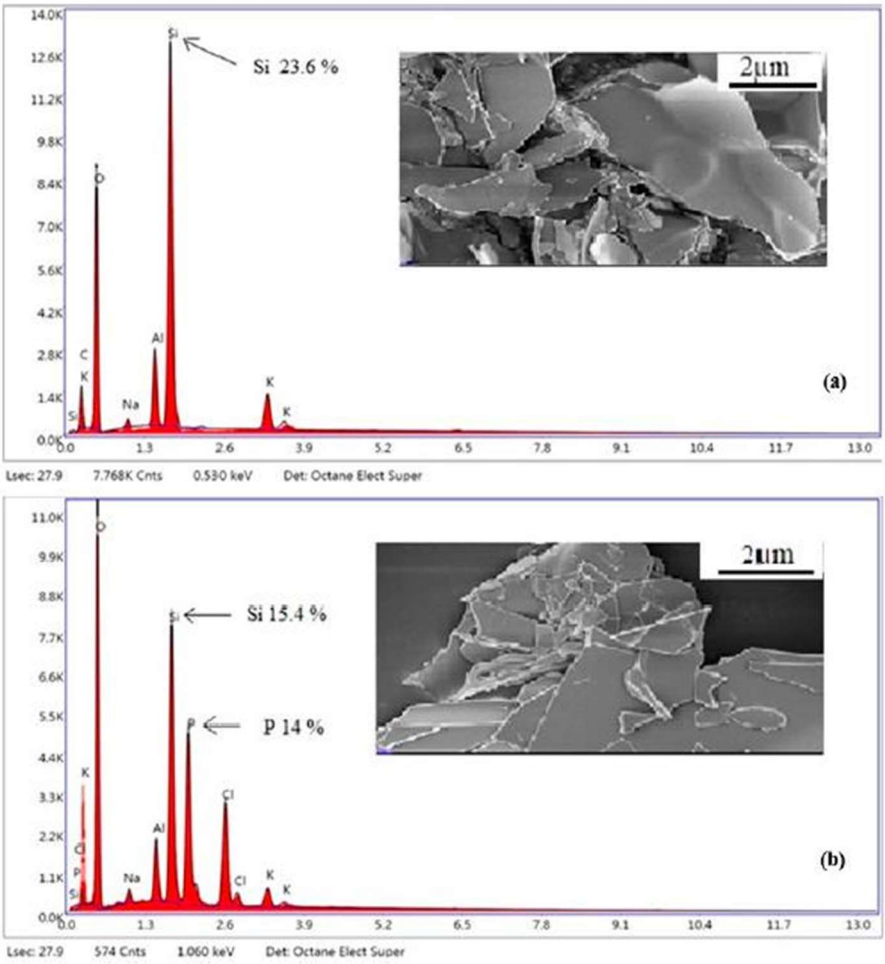

Fig. 5. SEM-EDX micrographs of EP (a) and PhEP (b)

According to the results of BET analysis, the nitrogen adsorption-desorption isotherm curve for both samples is of type 2 (Fig. 6). This indicates that both EP and PhEP samples have micro- and mesopores and the modification process does not affect the pore structure. The changes in surface properties given in Table 1 indicate that the surface of EP is modified during the OxCh reaction.

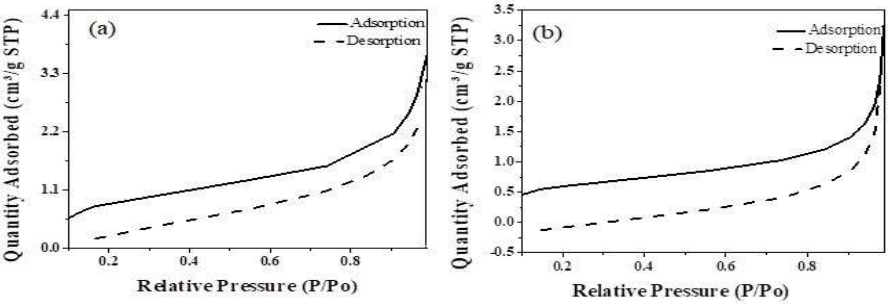

Fig. 6. N_2 adsorption-desorption isotherms at 77.4 K for EP (a), PhEP (b)

Table 1. Surface properties of EP and PhEP

Sample	Surface area (m^2/g)	Pore volume (cm^3/g)	Pore size (Å)
EP	3.2	0.0047	58.9
PhEP	2.05	0.0045	88.7

The TG curve of EP and PhEP is given in Figure 7.

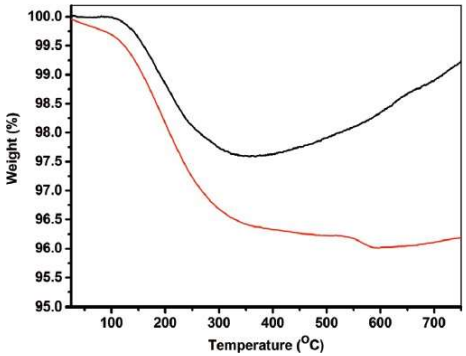

Fig. 7. TG curve of EP (black) and PhEP (red)

As can be seen from the figure, up to a temperature of 100 °C, PhEP has a greater mass loss (physically adsorbed water is released) compared to EP. This result can be explained by the presence of phosphorus-retaining groups in PhEP. In the subsequent temperature range (101–350 °C), the mass loss is up to 2.5%. At this stage,

phosphonic groups are dehydrated and dehydroxylation of silanol groups occurs. In the 3rd stage (after a temperature of 350 °C), PhEP has a mass loss of 2%. At this time, nitrogen is adsorbed in the pores and reacts with the silylene formed in the previous stage.

Figure 8 shows the dependence of the electrical conductivity (σ) of EP and PhEP on the logω parameter. Here ω is the angular frequency equal to $2\pi f$ with a frequency of f. The maximum σ of EP recorded at 1000 KHz was 0.35 S cm-1, while that of PhEP was 3.9 S cm-1 in the same range. The low conductivity of EP is due to its neutral nature (pH 6-8.5). The modification of the -P(O)(OH)2 groups in the EP structure provides more places for electrons to jump. Therefore, it leads to an increase in electrical conductivity at higher frequencies for PhEP.

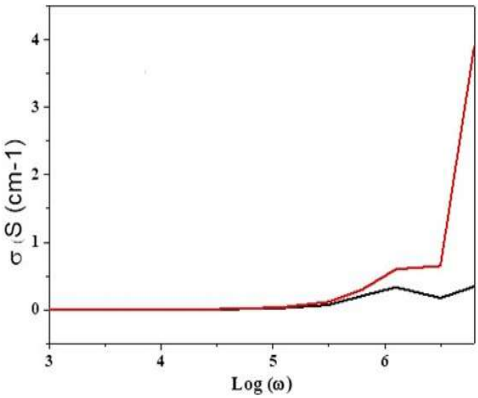

Fig. 8. Frequency dependence conductivity of EP (black) and PhEP (red)

In the second part of the third chapter, the structural features, thermal/electrical properties and kinetics of thermal degradation of PhBR, EP/PhBR, PhEP/PhBR and CB/PhBR samples were studied. For the synthesis of the samples, the OxCh reaction (the reaction was carried out with PCl_3 in an oxygen medium) was first applied. As is known, this reaction proceeds according to the free radical mechanism and begins with the formation of a chlorine radical. Then the chlorine atom acts on the BR and fillers.

For modified rubber (PhBR) and other samples (EP/PhBR, PhEP/PhBR, CB/PhBR), the following structures are likely to form after hydrolysis (Fig. 9).

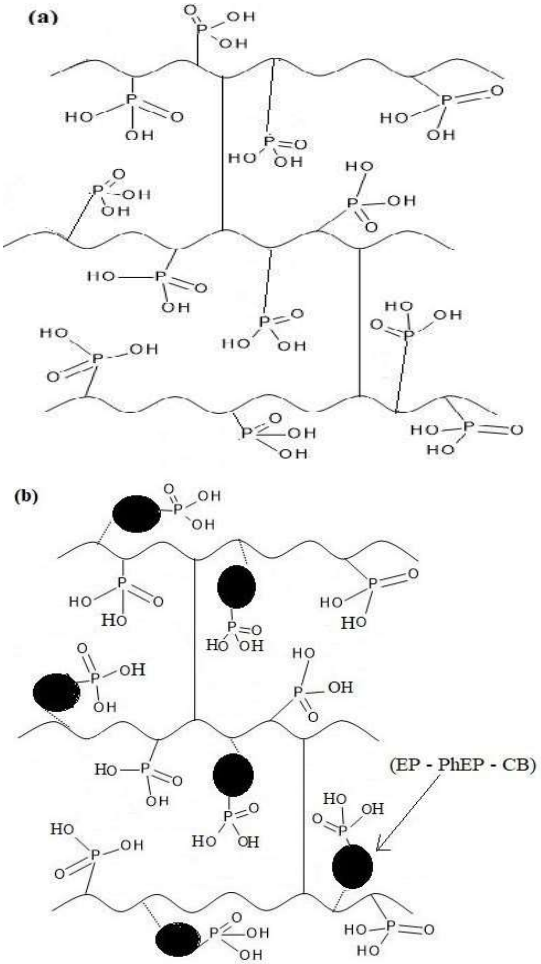

Fig. 9. The possible crosslink structure of PhBR (a), EP/PhBR, PhEP/PhBR, and CB/PhBR (b)

The static exchange capacity (SEC) of the samples was calculated, and the results are given in Table 2.

Table 2. Calculated SEC-s of modified BR and composites prepared on its basis

Sample	SEC (mq·eqv/g)
PhBR	12
EP/PhBR	13.6
PhEP/PhBR	12.96
CB/PhBR	12.3

As can be seen, the SEC parameter is relatively high in composites. This can be explained by the porous (or layered) structure of the fillers, which provide ion mobility in these composites, and a higher degree of swelling.

The structure of the samples was first studied by the FTIR spectroscopy method. The results are given in Figures 10 and 11.

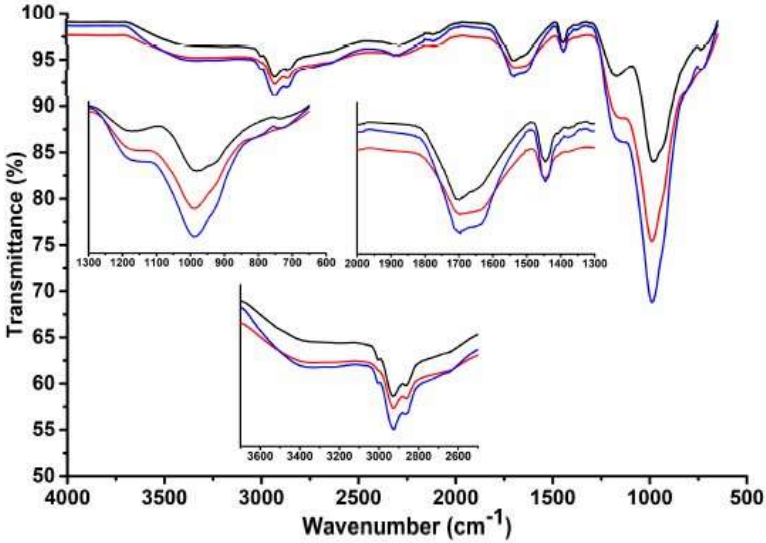

Fig. 10. FTIR spectra of PhBR (black), EP/PhBR (blue), and PhEP/PhBR (red) composites

The PhBR spectrum shows characteristic bands for the P=O functional groups at 1080 cm^{-1} and the −OH groups of the

−P(O)(OH)$_2$ at 1702, 2864 and 3394 cm^{-1}. The intense band at 986 cm^{-1}, which refers to the -C-O-P bond, indicates the attachment of the -P(O)(OH)$_2$ groups to the BR macromolecular chain through oxygen. The CH$_2$ groups of the rubber chain were observed at 1400– 1500 cm^{-1}. At first view, the FTIR spectra of the EP/PhBK and PhEP/PhBR composites appear similar to that of PhBR. This can be explained by the overlap of the characteristic bands of the -P-OH fragment and the -Si-O groups of EP. This indicates the formation of hydrogen bonds between the -Si-O and -P-OH groups as a result of the interaction between the PhBR and the fillers (EP/PhEP). The EP/PhBR band at 980–1000 cm^{-1} is more intense than the PhEP/PhBR band in the same range. This suggests that the interaction between PhEP and the modified rubber matrix (PhBR) is relatively strong in the PhEP/PhBR sample. In other words, the mineral is more uniformly distributed within the polymer matrix.

The CB/PhBR composite spectrum does not differ much from the PhBR spectrum. The FTIR spectra of the PhBR and CB/PhBR samples show only a slight increase in the intensity of the band at 982 cm^{-1} (Fig. 11).

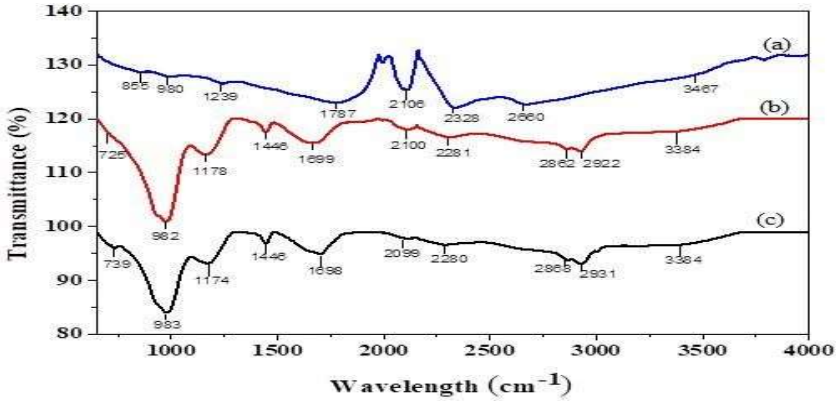

Fig. 11. FTIR spectra of CB (a), CB/PhBR Composite (b) and PhBR Matrix (c)

This result can be explained by the presence of a physical interaction between PhBR and CB. In the FTIR spectrum of pure CB (Fig. 11a), the bands at wavelengths 3467, 1239, 1787, 980 and

2016-2660 cm-1 are attributed to -OH, C-O, C=O, C=C-H and C-H fragments, which confirm the presence of carboxyl and hydroxyl groups in the sample. The indicated groups are sufficient for the interaction between CB and PhBR.

Comparative UV-vis spectra of PhBR with EP/PhBK, PhEP/PhBR and CB/PhBR (Fig. 12) show that fillers in composites affect the microscopic structure and Eg parameter of modified rubber (PhBR).

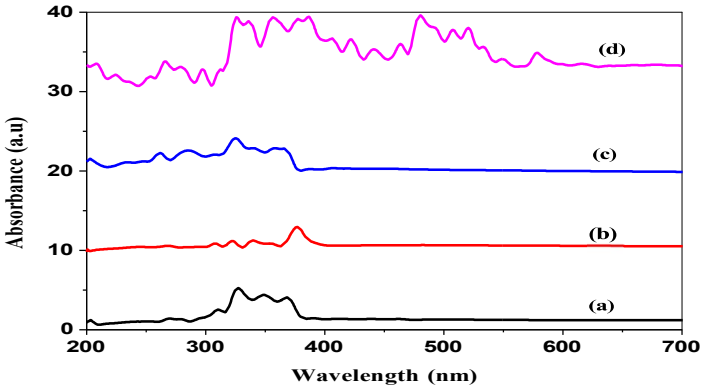

Fig. 12. UV-visible spectra of PhBR (a), EP/PhBR composite (b), PhEP/PhBR composites (c). and CB/PhBR composites (d)

As can be seen, in PhBR, broad UV absorption spectra of the π-π* connected BR system are visible in the interval 256÷390 nm. In composites, this band shifts to different ranges with the introduction of fillers (EP, PhEP, CB) into the PhBR structure. This result is associated with the formation of hydrogen bonds between PhBR and fillers due to functional groups in the prepared composites.

The values of Eg calculated directly and indirectly (using the Tauc equation) for the PhBR, EP/PhBR, PhEP/PhBR and CB/PhBR samples are shown in Figure 13. When EP and CB are introduced into the composites, the value of Eg decreases. This fact occurs as a result of some defects in the PhBR structure as a result of the dispersion/interaction of the fillers. In the PhEP/PhBR sample, the increase in Eg is due to the good dispersion and interaction of the PhEP filler in PhBR.

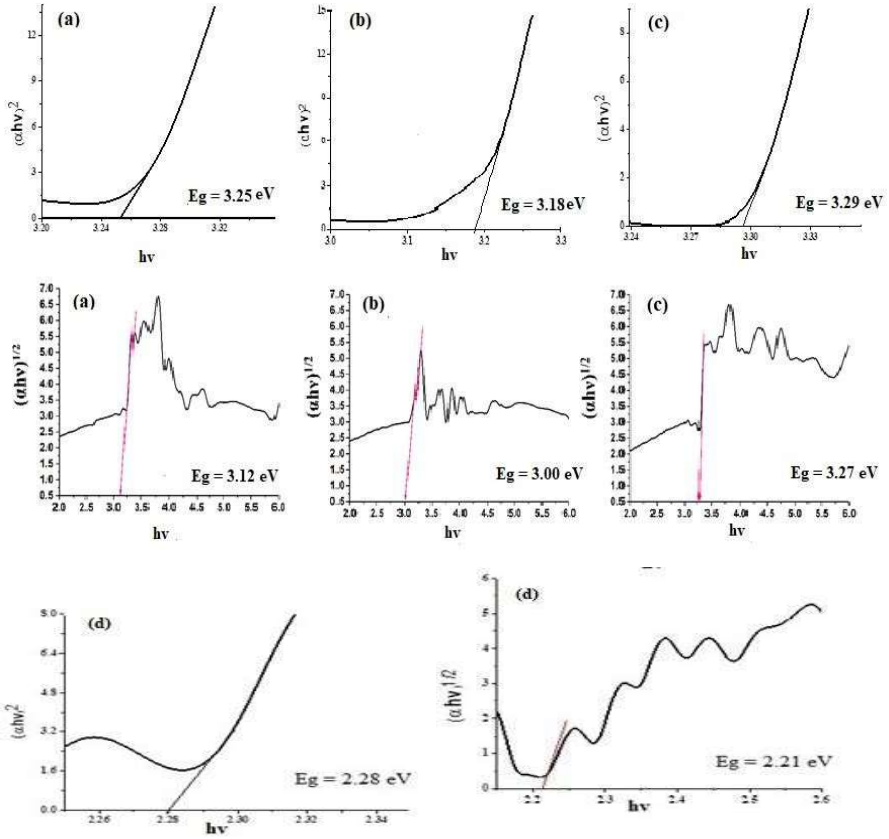

Fig. 13. The direct and indirect optical band gap calculations of PhBR (a,a), EP/PhBR (b,b), PhEP/PhBR (c,c), and CB/PhBR(d,d)

In the XRD measurements (Fig.14,15), the broad peak observed at 10°-40° 2θ for all samples (PhBR, EP/PhBR, PhEP/PhBR, CB/PhBR) indicates the amorphous phase. The increase in intensity in the EP/PhBR, PhEP/PhBR and CB/PhBR samples is a result of the formation of chemical bonds between PhBR and the fillers (EP, PhEP, CB). The peak is more intense in the PhEP/PhBR composite compared to EP/PhBR (Fig. 14). This result indicates a better dispersion of MEP in PhBR compared to GP due to the presence of - $P(O)(OH)_2$ groups on the surface of PhEP.

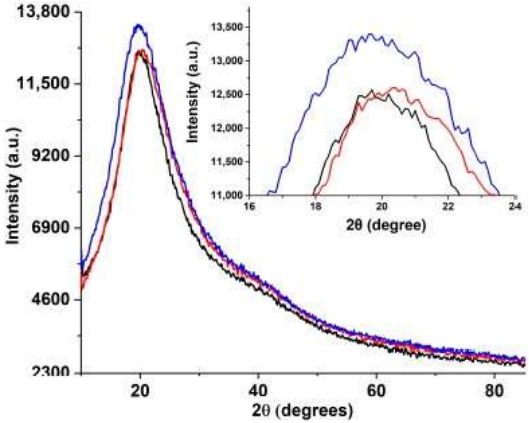

Fig. 14. XRD spectra of PhBR (black), EP/PhBR (red), and PhEP/PhBR (blue) composites

The high intensity of the corresponding peak in CB/PhBR (Fig. 15) indicates better interaction and dispersion of CB in the PhBR matrix. The disappearance of the characteristic peaks (002), (101) and (110) in the graphite-like structure of CB indicates intercalation interaction in the CB/PhBR sample.

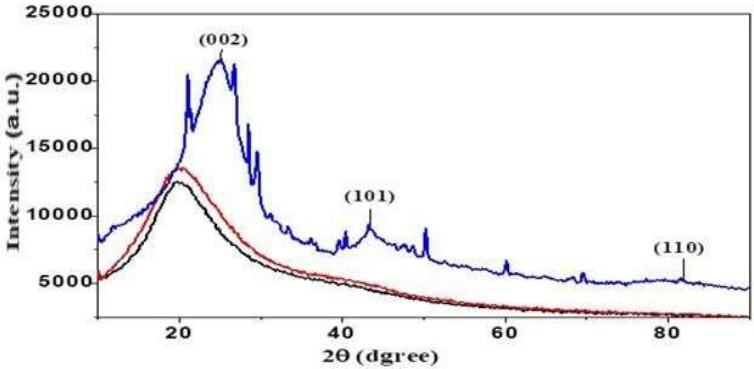

Fig. 15. XRD spectra of PhBR (black), CB (blue), and CB/PhBR (red) composites

Figure 16 shows the results of morphological and elemental analysis for all samples.

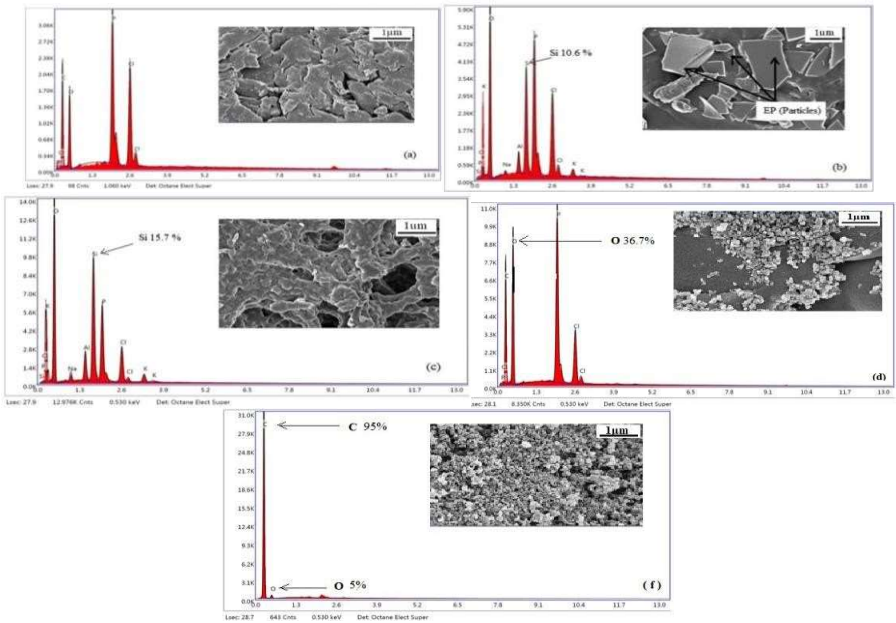

Fig. 16. SEM-EDX micrographs of PhBR (a), EP/PhBR composite (b), PhEP/PhBR (c), CB/PhBR (d), and CB (f)

As can be seen, unlike PhBR, EP/PhBR, PhEP/PhBR and CB/PhBR composites have 2 components: polymer matrix and fillers. The result for the PhEP/PhBR sample (Fig. 16c) shows a more even distribution of the components among themselves. This result is related to the good dispersion of PhEP in the polymer matrix due to the presence of -$P(O)(OH)_2$ groups on the surface of PhEP. In EP/PhBR (Figure 16b), the particles of EP in the PhBR matrix indicate poor dispersion in the matrix due to the low degree of modification. In the CB/PhBR composite, CB covering most of the PhBR surface indicates its good dispersion in the polymer matrix (Fig. 16d). Elemental analysis shows the presence of phosphorus for the corresponding samples. The presence of silicon in the EP/PhBR and PhEP/PhBR composites proves the modification of the polymer with EP. The higher content of silicon in PhEP/PhBR is related to the better distribution of PhEP in the polymer matrix. The relatively higher content of oxygen in EP/PhBR and PhEP/PhBR composites

compared to the CB/PhBR composite is due to the presence of SiO_2 in the EP samples.

In the next stage, the thermal stability of the composites and the modified polymer was studied comparatively. The results were evaluated by TG/DTG analysis in the range of 25÷750 °C (Fig. 17).

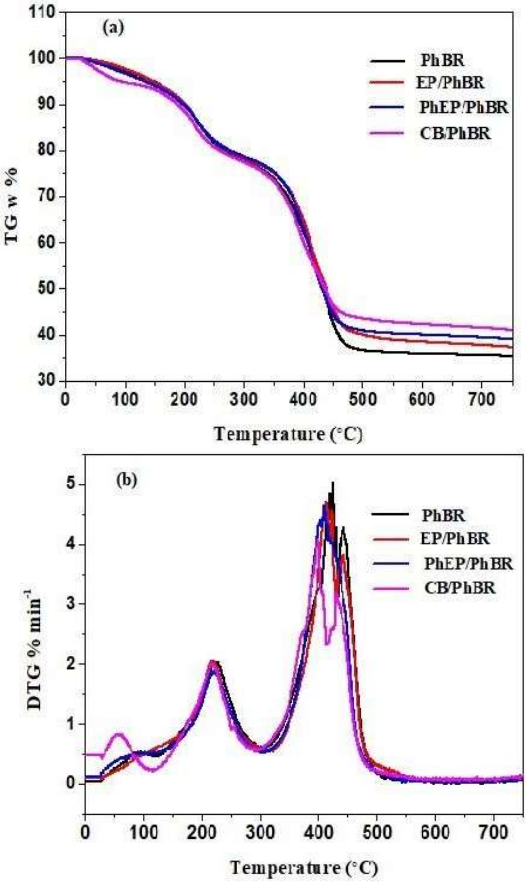

Fig. 17. TG/DTG curves of PhBR, EP/PhBR, PhEP/PhBR, and CB/PhBR

As can be seen, the process for all samples occurs in 3 stages. The first stage is the evaporation of physically adsorbed water, the second stage is the conversion of functional groups, and the third stage is the complete decomposition of the matrix.

As can be seen, the mass loss in EP/PhBR, PhEP/PhBR and CB/PhBR composites is less than that of PhBR. Based on the experimental results, the Decomposition Temperature Integration Procedure (DTIP) was calculated using the Doyles equation.

DTIP (^{O}C) = A* K* (T_f -T_i) + T_i,

where A* [(A1 + A2)/(A1 + A2 + A3)], K* is the coefficient [(A1 + A2) /A1], Ti and Tf are the initial and final temperatures of decomposition. A1, A2 and A3 are the areas visible in the TG curve (Fig.18).

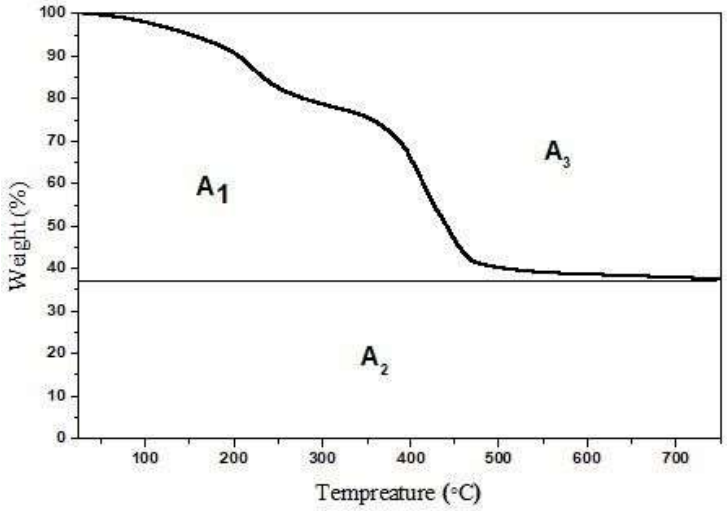

Fig. 18. Schematic representation of TGA area for calculation of DTIP values

It was determined that the thermal stability of the samples changes in the following sequence:

CB/PhBR > PhEP/PhBR > EP/PhBR >PhBR

The kinetics of thermal destruction of PhBR, EP/PhBR, PhEP/PhBR and EP/PhBR samples were studied using the Coats-Redfern method. Table 3 gives the activation energy values for the second and third stages of destruction.

Table 3. Kinetic parameters of thermal destruction of PhBR, EP/PhBR, PhEP/PhBR and CB/PhBR samples calculated according to the Coats-Redfern method

Sample	Second stage			
	n	R^2	E_a, kC/mol	log(A), 1/dəq
PhBR	1.5	0.9175	126	-11.4
EP/PhBR	2	0.9062	238	-0.54
PhEP/PhBR	1.5	0.9394	141.1	-10.2
CB/PhBR	1.5	0.9453	138	-10
	Third stage			
	n	R^2	Ea, kC/mol	log(A), 1/dəq
PhBR	4	0.9448	527.6	16.4
EP/PhBR	4	0.9429	478.1	12.2
PhEP/PhBR	4	0.9391	470.9	11.6
CB/PhBR	3.5	0.9395	342	1.4

The increase in Ea value in the second degradation stage of the EP/PhBR, PhEP/PhBR and /PhBR composite samples, compared to the PhBR sample, indicates that the fillers have been incorporated into the PhBR structure via the OxCh reaction. More energy is required to break down the composites' structure here. The cross- linked structure of PhBR means that the fillers affect the strength of the C-C bond, resulting in a higher energy requirement for decomposing the composites in the third stage. The different activation energies for the EP/PhBR, PhEP/PhBR and CB/PhBR composites are explained by the varying degrees of interaction between the fillers and the polymer matrix. Additionally, the kinetic parameters (E_a and A) of the thermal decomposition of the PhBR, EP/PhBR, and PhEP/PhBR samples, as well as the reaction mechanism of the thermal decomposition, were calculated using the model fitting method. The same results were obtained for the second and third decomposition stages (Table 4).

Table 4. Kinetic parameters calculated according to the reaction model of thermal destruction of PhBR, EP/PhBR and PhEP/PhBR samples

Sample	Second stage			Third stage		
	f(α)	E_a, kC/mol	lnA 1/min	f(α)	E_a, kC/mol	lnA 1/min
PhBR	F1.5	60.9	13.5	F3.5	245.1	44.7
EP/PhBR	F2	108	24.7	F4	224.4	39.5
PhEP/PhBR	F1.5	68.2	15.3	F4	217.7	39.5

In the next stage, PhBR, EP/PhBR, PhEP/PhBR and CB/PhBR samples were studied through BET analysis, and the results are presented in Figure 19.

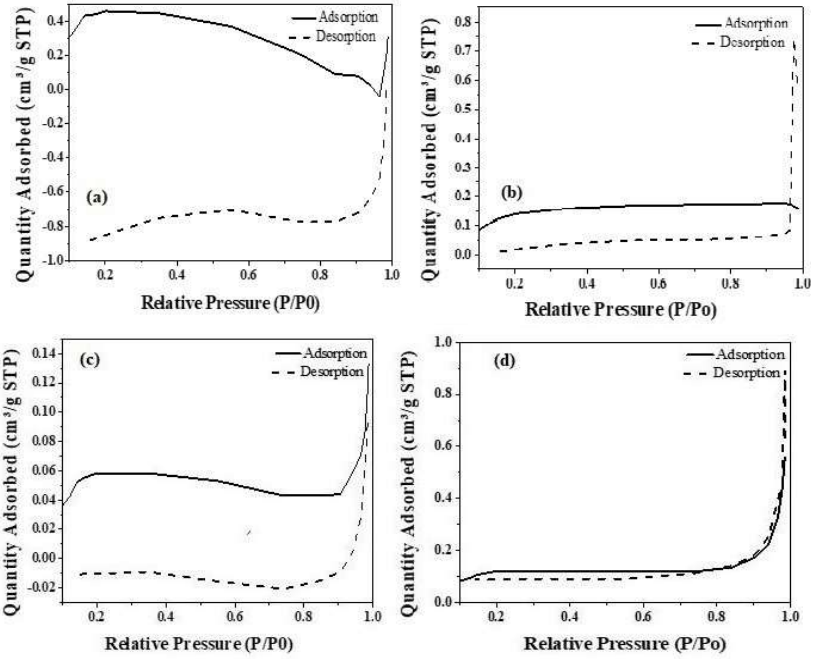

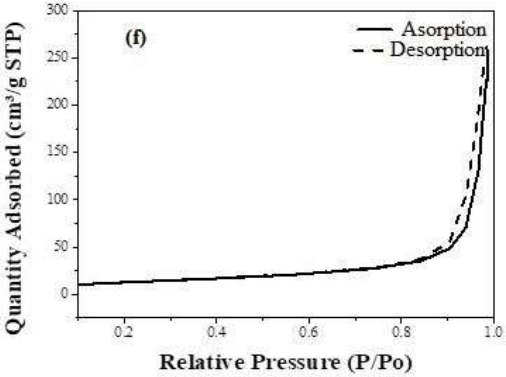

Fig. 19. N_2 adsorption-desorption isotherms at 77.4 K for PhBR (a), CB/PhBR (b), EP/PhBR (c), PhEP/PhBR (d), and CB(f)

Comparative studies allow us to determine the role of fillers in the three-dimensional spatial network of composites. As can be seen, the isotherm curves for all samples are of type II. These curves determine the micro- and mesoporous structure of the PhBR matrix, the change in surface area, the volume and size of pores, and the surface properties of the CB filler as a result of interaction with the fillers (Table 5).

Table 5. Surface properties of the PhBR, EP/PhBR, PhEP/PhBR, and CB/PhBR

Sample	Surface area (m^2/g)	Pore size (Å)	Pore volume (cm^3/g)
PhBR	1.3	9.6	0.000313
EP/PhBR	0.1743	41.3	0.000143
PhEP/PhBR	0.35	98.1	0.000866
CB/PhBR	0.5	19.92	0.000250
CB	46.0	303.7	0.34

The large distance between the adsorption and desorption curves of the PhBR sample indicates that the polymer macromolecules have mobility even after construction. This is associated with the low density of transverse bonds in the three-dimensional spatial network

structure. The decrease in the distance between the adsorption and desorption curves in the composites indicates that the fillers hinder the mobility of the macromolecule.

The effect of EP and PhEP fillers on the electrical properties of PhBR was studied from the point of view of electrical conductivity (σ) and dielectric permittivity (έ). Figure 20 shows the dependence of σ on log ω. Here ω is the angular frequency (equal to $2\pi f$, f is the frequency), and έ is calculated as follows:

$$\acute{\varepsilon} = {}^{C\,d}/_{A\,\varepsilon 0}$$

where έ is the dielectric constant, C is the capacitance of the sample (pF), d is the thickness of the sample (m), A is the area of the electrode (m2), ε0 is the dielectric constant in vacuum, 8.85 × 10-12 F m^{-1}.

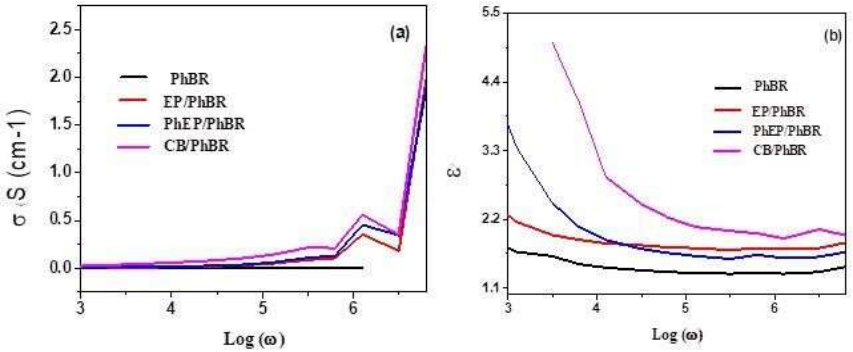

Fig. 20. Frequency dependence conductivity (a), and dielectric constant (b) of PhBR, EP/PhBR, PhEP/PhBR and C.B/PhBR composite

As can be seen, PhBR shows a conductivity plateau along the frequency range, as in insulating materials. This fact can be explained by the absence of a conduction path for charge carriers. In composites, the interaction of PhBR with EP, PhEP, CB provides a conduction path for charge jumps. As a result, the value of σ at 1000 kHz is 1.98 cm-1 (EP/PhBR), 1.87 cm^{-1} (PhEP/PhBR), 2.3 cm-1 (CB/PhBR) (Fig. 20a). A higher conductivity was obtained for the CB/PhBR sample, which is associated with the electrical properties

of CB. The layered structure of this filler enables tunneling/hopping of charges and consequently retains the electron transfer through the composite structure. Some of the occupied sites are due to the presence of -$P(O)(OH)_2$ groups in the PhEP sample. As a result, the σ value of PhEP/PhBR is reduced compared to EP/PhBR.

The dielectric properties of EP/PhBR, PhEP/PhBR and CB/PhBR composites compared to PhBR (Fig. 20b) are the result of the polarized system of the applied electric field and the fillers in the composites play the role of nanocapacitor. Also, the dielectrics belong to the Maxwell–Wagner–Sillars composites formed in the composites (Fig. 21). The dielectric properties of the composites are a good indicator of their high energy storage capacity.

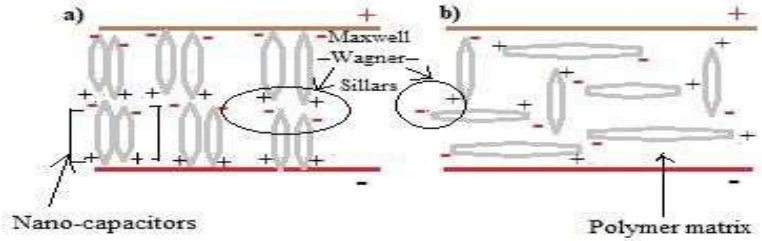

Fig. 21. Schematic representation of Maxwell–Wagner–Sillars polarization: (a) aligned systems and (b) randomly isolated system

In Chapter 4, the ability of PhBR polymer and various composites (EP/PhBR, PhEP/PhBR, CB/PhBR) to immobilize ZnS nanoparticles was compared. The SILAR method was applied to form nanoparticles, the presence of functional groups, the role of structural features of fillers was shown. The structure, electrical, bioactivity and photocatalytic properties of the prepared nanocomposites (ZnS/PhBR, ZnS/EP-PhBR, ZnS/PhEP-PhBR, ZnS/CB-PhBR) were studied in detail.

The probable mechanism of ZnS nanoparticles formation in matrices is shown (Fig. 22). Here, the role of functional groups in the formation of nanoparticles is shown. When $ZnCl_2$ solution is added to the polymer and composites, Zn^{2+} ions are adsorbed due to the

functional groups, and then ZnS nanoparticles are formed when they come into contact with Na_2S solution.

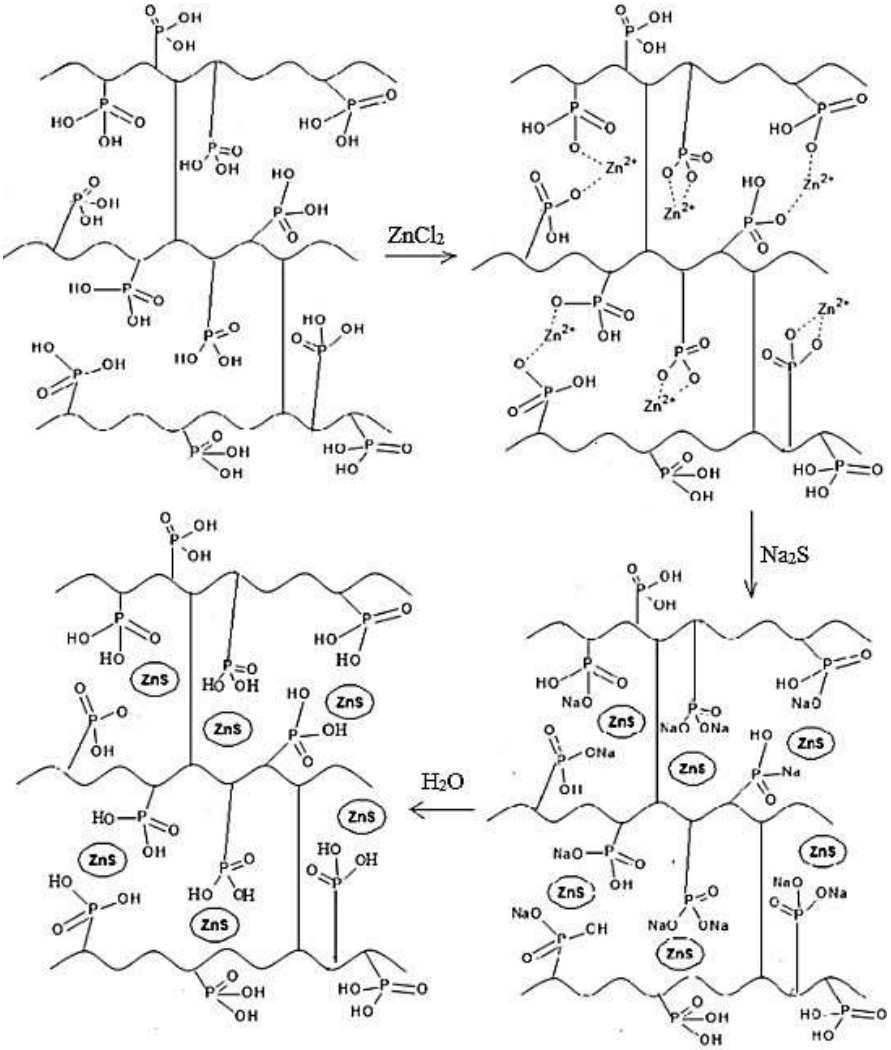

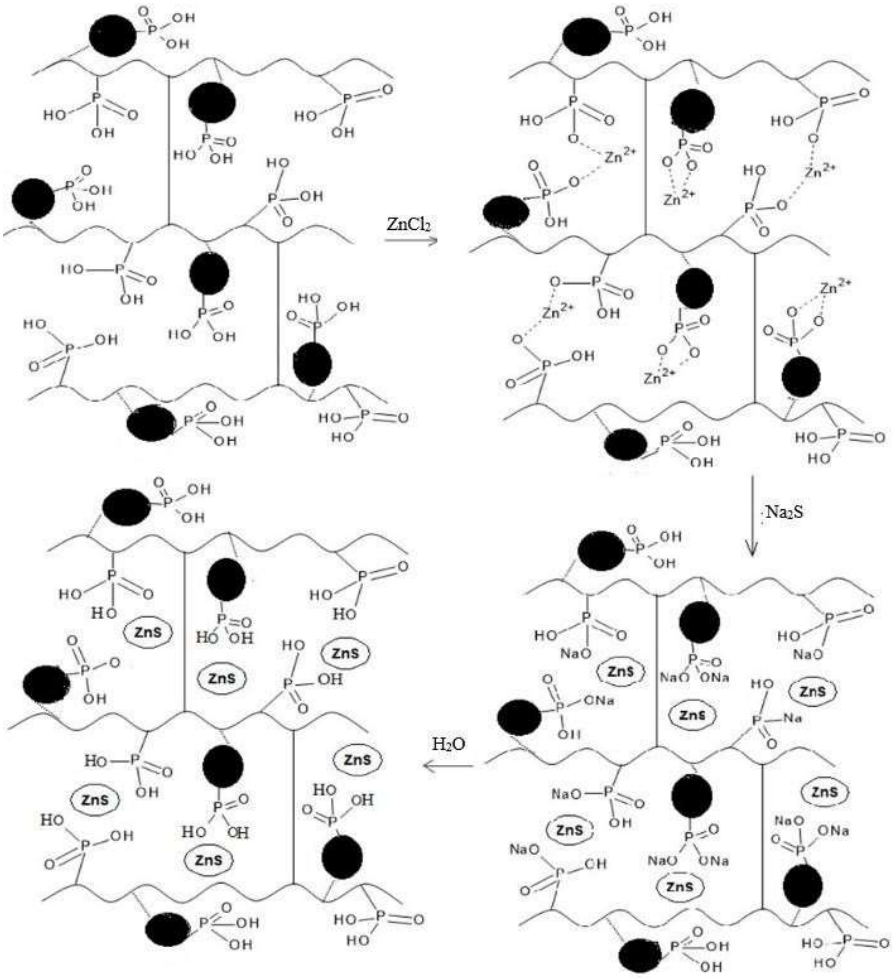

Fig. 22. SILAR reaction mechanism of ZnS/nanocomposites preparation

The color of the obtained polymers and composites was compared with the color of the nanocomposites prepared on their basis, as well as with the color of "pure" ZnS. The color change indicates the presence of ZnS in the samples.

PhBR, composites and nanocomposites prepared on their basis were studied by UV-vis spectroscopy, the corresponding spectra are

given in Figure 23 for comparison with the composite and nanocomposite prepared on the basis of CB.

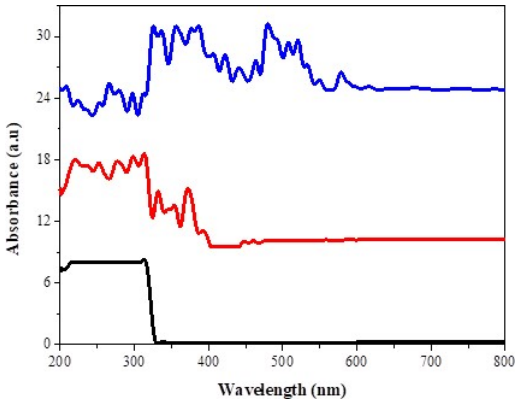

Fig. 23. UV-vis spectra of CB/PhBR (blue), nanocomposite (red) and "pure" ZnS

The corresponding shifts in the spectrum of the nanocomposite compared to the original sample indicate the interaction of the ZnS nanoparticles with the matrix. Table 6 gives the band gap width for all samples.

Table 6. Comparative Eg values of PhBR composites and their ZnS/nanocomposite

Samlpes	**E_g (eV)**
PhBR ZnS/PhBR	3.25 3.78
EP/PhBR ZnS/EP-PhBR	3.18 3.032
PhEP/PhBR ZnS/PhEP-PhBR	3.29 2.9
CB/PhBR ZnS/CB-PhBR	2.28 3.83
ZnS	3.8

As can be seen, the immobilization of ZnS nanoparticles in EP/PhBR and PhEP/PhBR composites results in a decrease in the Eg parameter. The reason for this is that the filler (EP) used in the preparation of the indicated composites has a porous structure, ions easily diffuse into it, and as a result, nanoparticles are formed inside. When ZnS nanoparticles are immobilized in PhBR and CB/PhBR samples, the Eg parameter of the obtained nanocomposites increases. The reason for this is that ZnS nanoparticles are mainly formed on the surface.

The prepared samples (composite and nanocomposites) were also studied by the RFA method. The results are shown in Figure 24 for the example of EP/PhBR and the nanocomposite prepared on its basis. The peaks at 30°, 48° and 56° on the 2θ axis indicate the cubic shape of the formed ZnS nanoparticles.

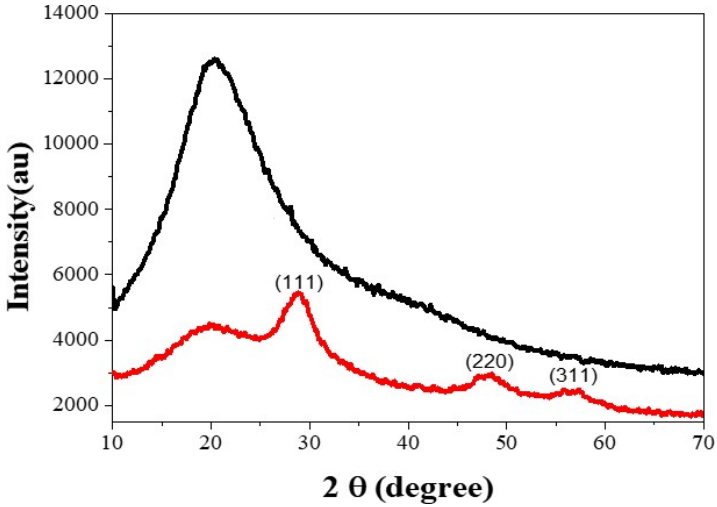

Fig. 24. Diffractograms of EP/PhBK (black color) and ZnS/EP-PhBR (red color)

In addition, after immobilization of ZnS nanoparticles, the decrease in the intensity of the broad peak corresponding to polymers and composites and the appearance of a new peak corresponding to ZnS confirm the immobilization process. Table 7 shows the

calculated dimensions for the characteristic peaks ((111), (220), (311)) corresponding to ZnS nanoparticles:

$$D = \frac{K\lambda}{\beta cos\theta}$$

Where D is the crystal size, K is the particle shape factor (0.94), β is the full width at half maximum (FWHM), θ is the Bragg angle, and λ is the X-ray wavelength (1.54056 Å)

Table 7. *D* parameter of the ZnS/nanocomposites determined by the Debye-Scherrer equation

ZnS/nanocomposite	Particle size (nm)
ZnS/PhBR	3
ZnS/EP-PhBR	3
ZnS/PhEP-PhBR	8
ZnS/CB-PhBR	3

In order to determine the interaction of ZnS nanoparticles with the composites in the prepared nanocomposites, the electrical conductivity of the samples was studied. The results are given in Table 8.

Table 8. Comparative conductivity (σ) values of PhBR composites and their ZnS/nanocomposite

Samples	Conductivity (σ)
PhBR	0.00
ZnS/PhBR	0.06
EP-PhBR	1.98
ZnS/EP-PhBR	3.38
PhEP-PhBR	1.87
ZnS/PhEP-PhBR	2.28
CB-PhBR	2.34
ZnS/CB-PhBR	0.83

As a result of the immobilization of ZnS nanoparticles in EP/PhBR and PhEP/PhBR composites, the value of σ increases significantly due to electrical conductivity. A slight increase in the

value of σ when ZnS particles are formed in the PhBR polymer indicates a weak interaction between the matrix and the particle. In the case of the formation of nanoparticles in the CB/PhBR composite, the σ parameter of the nanocomposite decreases. This is due to the formation of ZnS nanoparticles on the surface and the interruption of the conductivity chain in the CB filler. In nanocomposites, due to the interaction of the particle with the matrix, polarized ions are isolated and the dielectric properties (έ) are disturbed. The increase in έ in ZnS/PhBR is explained by the transition of PhBR from an isolated form to a conductive form due to immobilization.

Chapter 5 tested the antibacterial activity of the samples against Gram-positive (+G) and Gram-negative (-G) bacteria. The results showed that the PhBK sample exhibited good antimicrobial activity, which can be attributed to the presence of phosphorus-containing acid groups and chlorine atoms in the polymer, and their strong interaction with bacteria. However, in composites and nanocomposites prepared using this polymer, the functional groups are captured by ZnS particles and the antibacterial activity decreases. Since 'pure' ZnS is sufficiently mobile, it can easily enter bacterial cells, generate active oxygen, and destroy the bacteria (Fig. 25).

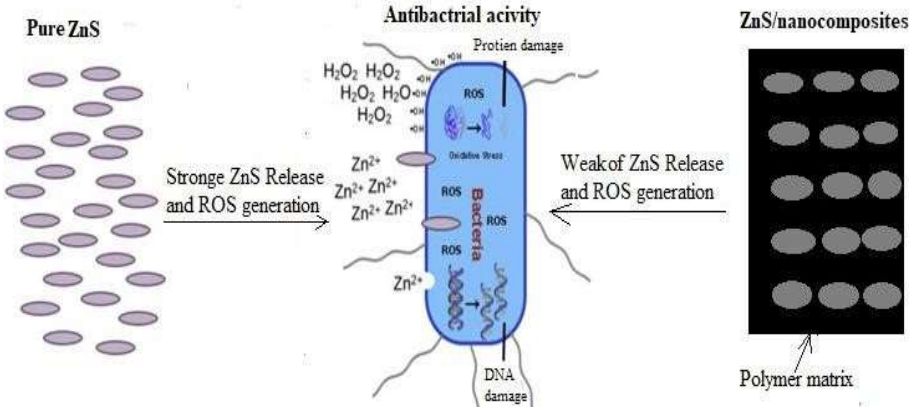

Fig. 25. Antibacterial activity of pure ZnS and immobilized ZnS in ZnS/PhBR, ZnS/EP-PhBR, ZnS/PhEP-PhBR, ZnS/CB-PhBR nanocomposites

Since ZnS particles are strongly bound to the matrix in the composite, they cannot enter bacterial cells, resulting in lower antibacterial activity of the nanocomposites compared to “pure” ZnS.

The next stage involved studying the photocatalytic decomposition of crystal violet dye (CV) under visible light from a tungsten lamp. The catalysts used were “pure” ZnS, polymer (PhBR) composites (EP-PhBR, PhEP-PhBR and CB-PhBR), and nanocomposites (ZnS/PhBR, ZnS/EP-PhBR, ZnS/PhEP-PhBR and ZnS/CB-PhBR). The results are given in Table 9.

Table 9. Photocatalysis oxidation of CV PhBR composites, ZnS/nanocomposites, and pure ZnS

Sample	0 min	15 min	30 min	45 min
CV 0.02 mmole	11 %	35%	30%	23.5%
PhBR	11 %	50%	72%	85.5%
ZnS/PhBR	11 %	76%	78%	88.5%
EP/PhBR	11 %	70%	80%	83.5%
ZnS/EP-PhBR	11 %	81.5%	87%	95.5%
PhEP/PhBR	11 %	91.5%	96.5%	98.2%
ZnS/PhEP-PhBR	11 %	77.5%	83%	90%
CB/PhBR	11 %	75%	82%	94%
ZnS/CB/PhBR	11 %	87.8%	91.15%	97%
Pure ZnS	11 %	64%	63%	60%

During photooxidation, electrons are excited and transferred from the valence band to the conduction band of ZnS. This results in the formation of electron-hole pairs. Free radicals are formed through interaction with electron pairs in the environment, resulting in dye oxidation (Fig. 26).

Using nanocomposites as catalysts causes CV to decompose more. In this case, the composite matrix ensures that the ZnS particles remain at the nanoscale. However, when "pure" ZnS is used, its photocatalytic activity decreases due to agglomeration.

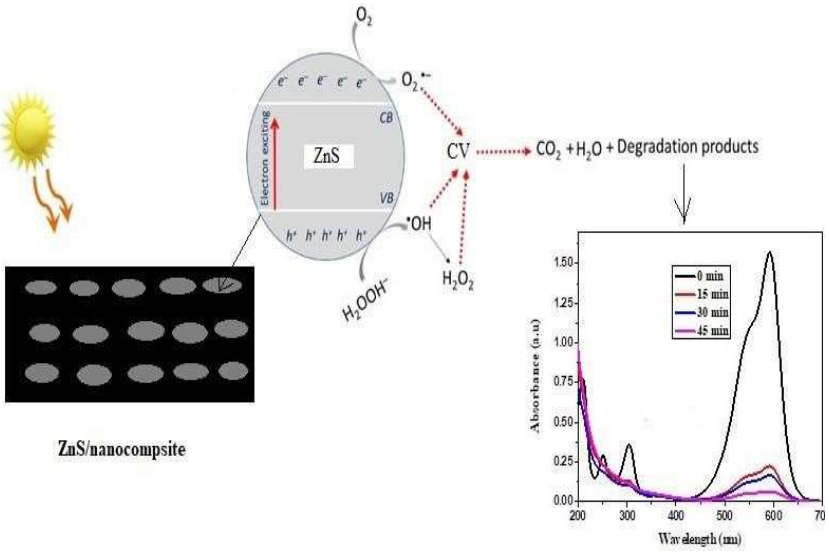

Fig. 26. Photocatalysis oxidation mechanism of CV by ZnS (Pure/immobilized ZnS in composite)

The different results obtained with nanocomposites based on different matrices can be explained by the ZnS particle dispersion degree. ZnS/CB-PhBR showed the highest efficiency, which can be attributed to the high degree of particle dispersion in this sample. During experiments with PhBR, EP/PhBR, PhEP/PhBR and CB/PhBR samples, the decrease in CV concentration in the solution is due to adsorption resulting from chemical and physical interactions. Studies with PhBR, EP/PhBR, PhEP/PhBR and CB/PhBR samples indicate that the pH value varies within the range 2–5, which suggests that dye substance concentration occurs due to adsorption. In nanocomposites, the pH value varies within the range 6–7. The decomposition products of CV do not absorb light. When "pure" ZnS is used, particle agglomeration occurs and the decomposition rate decreases (Table 9, Fig. 27).

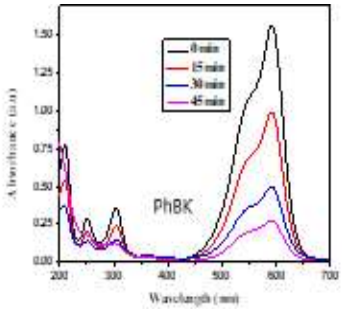
0 min
15 min
30 min
45 min
PhBK
Absorbance (a.u)
Wavelength (nm)

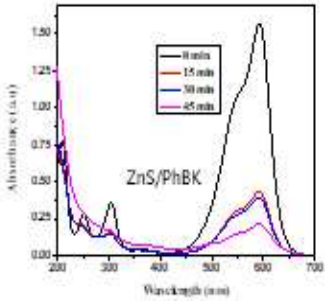
0 min
15 min
30 min
45 min
ZnS/PhBK
Absorbance (a.u)
Wavelength (nm)

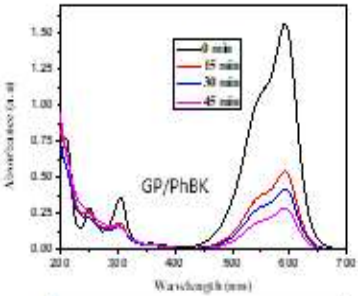
0 min
15 min
30 min
45 min
GP/PhBK
Absorbance (a.u)
Wavelength (nm)

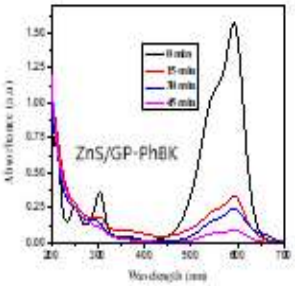
0 min
15 min
30 min
45 min
ZnS/GP-PhBK
Absorbance (a.u)
Wavelength (nm)

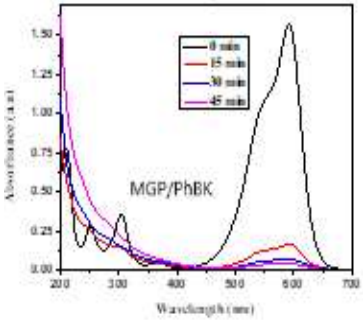
0 min
15 min
30 min
45 min
MGP/PhBK
Absorbance (a.u)
Wavelength (nm)

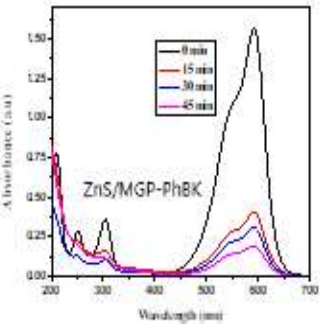
0 min
15 min
30 min
45 min
ZnS/MGP-PhBK
Absorbance (a.u)
Wavelength (nm)

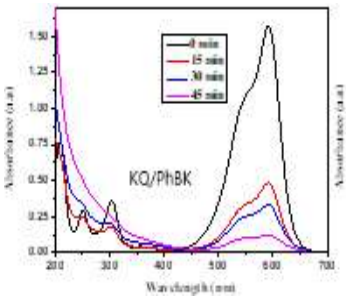
0 min
15 min
30 min
45 min
KQ/PhBK
Absorbance (a.u)
Wavelength (nm)

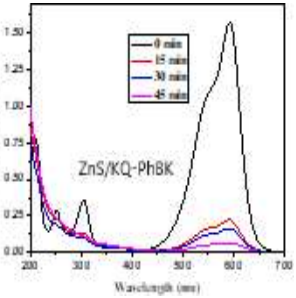
0 min
15 min
30 min
45 min
ZnS/KQ-PhBK
Absorbance (a.u)
Wavelength (nm)

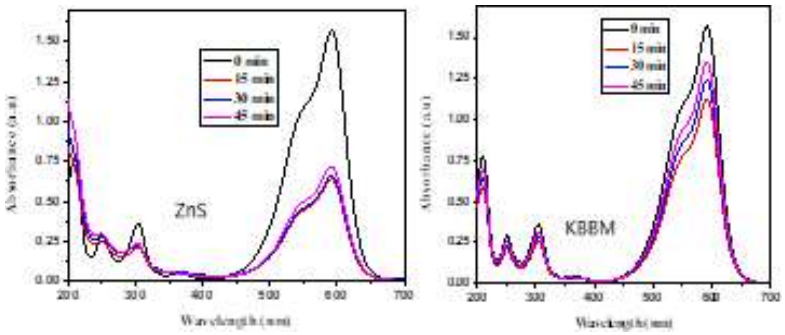

Fig. 27. Photocatalysis oxidation of CV, PhBR composites, ZnS/nanocomposites, and pure ZnS under visible light using a tungsten lamp

CONCLUSIONS

1. For the first time polymer composites of BR with mineral filler as EP (pure and modified) and CB were prepared joining the OxCh using PCl_3 and O_2. Three different structures of the rubber composites were obtained: EP/PhBR, PhEP/PhBR, and CB/PhBR.

2. Synthesis of the PhBR and PhEP were carried out separately using OxCh reaction for comparison purposes. Both compounds were obtained by subsequent hydrolysis of the final products. The structure of the PhEP was carefully analyzed in comparison to the EP. The FTIR, UV-Vis spectra show the intermolecular interaction of the Si-OH groups of EP with (-P(O)$(OH)_2$) confirming the modification of the EP surface with phosphorus acid groups, this result supported by EDX plot of PhEP that show 14% of the P atoms. Alter in Eg energy of EP also assigns the effects of the (-P(O)$(OH)_2$) on the optical properties of the EP. The BET, SEM, TG/DTG analyses, and using the Capacitance Resistance meter for electrical properties measurements observed changes in the surface properties, morphology and thermal/ electrical properties of EP concerning the modification with phosphorus acid groups (-P(O)$(OH)_2$).

3. The final form of the polymer composites products (EP/PhBR, PhEP/PhBR, CB/PhBR, and PhBR) were obtained by subsequent hydrolysis of the solid products obtained in the reaction medium. A free radical mechanism was adopted as the only reaction mechanism

for intermolecular interaction between the precursors (rubber–fillers) to build up the cross-link structure of the polymer composites. For the synthesis of the composites, the fillers were added in a ratio of 1:5 (BR: fillers). The exothermic nature of the reaction and the mild stirring were found to be the optimum reaction conditions for the filler-rubber interaction. The pores structure and moieties of the fillers play a special role in the interaction and develop the crosslink structures of the polymer composites. OxCh reaction of PhBR and PhEP was exothermic character proceeded through a free radical mechanism too. The structures and chemical composition of the polymer composites were attentively studied using FTIR, UV-Vis, and EDS. Comparative FTIR spectrums of the phosphorylated butadiene rubber with/without fillers shows the real intermolecular chemical interaction of modified rubber (PhBR) and fillers in the three prepared composites (EP/PhBR, PhEP/PhBR, and CB/PhBR). The effect of the fillers on the optical properties and microscopic structure of the modified rubber was given by UV measurement of the composites. Elemental analysis by EDS observes the modification of rubber with phosphoric acid groups due to the appearance of the P atom in the EDS plot of PhBR, a considerable percentage of Si atom in case EP/PhBR and PhEP/PhBR and the high amount of the C atom in CB/PhBR assign the incorporation of the expanded perlite and carbon black fillers within the structure of modified rubber.

4. Topography of the EP/PhBR, PhEP/PhBR, and CB/PhBR analyzed by SEM, the images show heterogenous and homogenous phases which reflected the dispersion degree of the fillers on the rubber matrix. The homogenous phase of PhEP/PhBR reflects the high dispersion degree and affinity of the PhEP to interact with PhBR due to the presence of the phosphoric acid groups on the surface of the PhEP. Phase structure analysis using XRD a new amorphous phase structure for all PNCs in comparison to the PhBR. Calculation of the thermal stability parameters using the Coats-Redfern method shows a decrease of the E_a for the second and third stages of the thermal degradation of the EP/PhBR, PhEP/PhBR, and CB/PhBR in comparison to the PhBR. This result assigns the effect of the fillers on the cross-linked structure of the modified rubber matrix and their

contribution to the thermal stability of modified rubber composites. The surface structure parameters of PNCs were studied by BET analysis. The change in the pore size/volume and surface area of rubber observed the contribution of the fillers in designing the cross- link structure of composites. Moreover, the N_2 absorption and desorption curves of composites shows the different dispersion degrees of the fillers on the rubber matrix. Based on the electrical properties study of the EP/PhBR, PhEP/PhBR, and CB/PhBR, the conductivity and dielectric curves show the contribution of the interacted fillers in obtaining continuous hopping of charges over the rubber matrix in all composites this phenomenon was clear in the CB/PhBR due to the electric conductive properties of the CB that have graphite-like structure.

5. Applying the SILAR method in three cycles succeeded in immobilizing the ZnS nanoparticles in the composite structures and obtaining ZnS/EP/PhBR, ZnS/PhEP/PhBR, ZnSCB/PhBR, and ZnS/PhBR nanocomposites. The meso/micro cross-link structures of the composites helped to enough swelling of the EP/PhBR, PhEP/PhBR, and CB/PhBR structures in the $ZnCl_2$ and Na_2S solutions which allowed the diffusion and immobilizing of the ions into crosslink structure while the suppressed PhBR structure restricted the diffusion of the ions. The phosphoric acid groups in the composite structures allowed in-situ reduction of the zinc ions. The ZnS particles were found trapped on the blocked structure of the polymer composites through intermolecular hydrogen bonds with (- $P(O)(OH)_2$. The pores structure of the EP, PhEP, and CB fillers assisted the swelling of the polymer composites obtaining more diffusion of the ions moreover, the moieties on the filler's surfaces also included in-situ reduction of the Zn ions which effectively assisted the dispersion of the ZnS nanoparticles over polymer composites structures.

6. Change in optical properties of PNCs and PhBR composites after immobilizing the ZnS nanoparticles indicate the intermolecular interaction of the ZnS nanoparticles with the composite structures. Based on the XRD analysis of the prepared PNCs it was found that the polymer composites stabilized cubic phase structure of ZnS with

3 nm in case of the EP/PhBR, CB/PhBR, and PhBR, while the PhEP/PhBR immobilized ZnS of 8 nm size. Immobilize ZnS show an increase in the conductivity and dielectric properties of the PhBR, EP-PhBR, and PhEP-PhBR, this result was attributed to the increase of intermolecular components, enhanced degree of crystallinity, and formation of the charge-transfer, while the opposite obtained in the CB/PhBR due to high load of deposited ZnS on the CB/PhBR, especially on the CB structure that disruption and cut off the flow of the charges.

7. The composites and PhBR succeeded in the immobilization of ZnS nanoparticles and attained the desired control of structure/size and well dispersion of the ZnS nanoparticles on composites, and increased the ZnS photocatalysis activity, thus the PNCs show a higher percentage of CV degradation rate due to the large redox surface offered by the ZnS nanocomposites in comparison to the agglomerated pure ZnS particles. The lower antibacterial activity of the PNCs in contract to the composites and PhBR confirm the strong intermolecular interaction of the ZnS nanoparticles with the composite structures that locked the antimicrobic property of the composites due to ZnS - phosphorus acid groups interaction.

8. The strong stacking of the ZnS in composite structures decreases the availability of the ZnS in the bacterial medium and reduces the production of reactive oxygen species that can cause bacterial death, while the pure ZnS was free to diffuse through the cell membrane and highly produced active oxygen species that cause bacterial death. The new PNCs prepared in this dissertation also can be suggested for various ZnS applications such as sensor, energy storage, and hydrogen generation and others ZnS applications. The new filler/polymer matrix prepared in dissertation can be used to immobilize other nanoparticles than ZnS. The new matrix prepared in this dissertation can be suggested for other applications than to be used as a NPs stabilizer for example they can be suggested as an adsorbent or flame retardant material.

Published scientific works on the topic of the dissertation

1. Edres, N., Buniyat-zadeh, I.A., Alosmanov, R.M Chemical Modification of Expanded Perlite by Oxidative Chlorophosphorylation Reaction // International Ankara Congress on Scientific Research IV. Ankara, Turkey, − 2022, − p. 1045.
2. Edres, N., Buniyat-zadeh, I.A, Alosmanov, R.M. Functionalization of carbon black surface with phosphorus acid group (–P(O)(OH)2) through Oxidative Chlorophosphorylation // ASES International Health, Engineering and Sciences Congress. Ankara, Turkey, − 2022, − p. 302.
3. Edres, N., Buniyat-zadeh, I.A., Turp, S. M., Alosmanov, R.M. Synthesis and Characterization of Phosphorus – Containing Butadiene Rubber / Expanded perlite Composite // V International (XV Ukrainian) conference. Vinnytsia, Ukraine, −2022, − p. 156.
4. Edres, N., Buniyat-zadeh, I.A., Alosmanov, R.M. Investigation Structure of Expanded Perlite Phosphorus - Containing Butadiene Rubber Hybrid Composite // International Conference of Modern Problems of Theoretical and Experimental Chemistry. Baku, Azerbaijan, − 2022,− p.230- 231.
5. Edres, N., Buniyat-zadeh, I.A., Turp, S. M., Alosmanov, R.M. Synthesis and characterization of phosphorus-containing Butadiene rubber/expanded perlite composite// International Ankara Congress on Scientific Research IV. Ankara, Turkey, −2022, − p. 1042.
6. Muradov R., Edres N., Alosmanov R. Adsorption of crystal violet dye with expanded perlite and butadiene rubber/expanded perlite based composite // Ümummilli Lider Heydər Əliyevin anadan olmasının 99-cu ildönümünə həsr olunmuş doktorant, magistrant və gənc tədqiqatçıların "Kimya və Kimya Texnologiyası" mövzusunda Respublika Elmi Konfransı, – Bakı: – 18 – 19 May, – 2022, – p. 404.

7. Edres, N. Structural Characterization of Composites Based on Butadiene Rubber and Expanded Perlite / Nada Edres, Irada Buniyat-zadeh, Rasim Alosmanov [et. al.] // Journal of Composites Sciences, −2023. 7(12). − p. 487-504.
8. Edres, N., Buniyat-zadeh, I., Alosmanov, R. Oxidative chlorophosphorylation reaction - carbon black/modified butadiene rubber composite / Investigation structure // Мавзусидаги халқаро илмий-амалийконференция-Функци- онал полимерларнинг фундаментал ва амалий жиҳатлари. Тошкент, Uzbekistan,−2023, − p. 516-518.
9. Edres, N. Structure and thermal stability of phosphochlorinated polybutadiene/carbon black composite synthesized via oxidative chlorophosphorylation reaction / Nada Edres, Solmaz Aliyeva, Sinan Turp [et al.] // Journal of the Serbian Chemical Society, - 2023. 89(1). − p. 79 -190.
10. Edres, N., Buniyat-zadeh, I., Turp, S. M., Alosmanov, R., Soylak, M. Morphological structure study of butadiene rubber/expanded perlite composite: Effect of modification // Tokyo 7th international innovative studies and contemporary scientific research congress. Tokyo, Japan,−2023,− p.1135- 1136.
11. Edres, N., Buniyat-zadeh, I.A., Alosmanov, R.M. Oxidative chlorophosphorylation reaction-carbon black/phosphorus-containing butadiene rubber composite: Thermal stability study // Ümummilli Lider Heydər Əliyevin anadan olmasının 100-cü ildönümünə həsr olunmuş doktorant, magistr və gənc tədqiqatçıların «Kimya və Kimya Texnologiyası» II Respublika Elmi Konfransı, − Bakı: − 4 − 5 May, − 2023, − p. 60-61.
12. Edres, N., Buniyat-zadeh, I., Eyvazova, G., Mammadyarova, S., Alosmanov, R. Stabilization of ZnS nanoparticles based on modified butadiene rubber/expanded perlite and carbon black composites: structure, optical and conductivity properties // The 8th International conference modern trends in physics, Baku, Azerbaijan, – 2023, – p.176-177.

13. Edres, N. Thermal Degradation Kinetic Study of Expanded Perlite-Modified Butadiene Rubber Composites / Nada Edres, Solmaz Aliyeva, Rasim Alosmanov [et al.] // Macromolecular Reaction Engineering, – 2024. 18 (5), – p. 240005.
14. Edres, N. Study of structure and electrical-/dielectric properties relationship of butadiene rubber-/carbonblack hybrid composite / Nada Edres, Nurlana Binnetova, Rasim Alosmanov [et al.] // Azerbaijan chemical journal, – 2024. 3, – p. 94-101.
15. Edres, N. Growing ZnS nanoparticles on novel expanded perlite-butadiene rubber composite by SILAR method / Nada Edres, Goncha Eyvazova, Sevinj Mammadyarova [et al.] // Journal of Rubber Research, – 2024. 27 (3), – p.299-308.
16. Edres N., Buniyat-zadeh I., Suleymanova T., Alosmanov R. Anti-bacterial activity of ZnS/ expanded perlite phosphorylated butadiene rubber nanocomposite // 22nd Mendeleev Congress on general and applied chemistry. Sochi, Russia, – 2024, – p.107.

The defense will be held on 22 September 2025 at 11^{00} at the meeting of the Dissertation Council BED 2.16 of Supreme Attestation Comission under the President of the Republic of Azerbaijan at Baku State University.

Address: Baku city, Zahid Khalilov street, main building AZ 1148.

Dissertation is accessible at the Baku State University Library.

Electronic version of the abstract is available on the official website of Baku State University.

Abstract was sent to the required addresses on 14 July 2025.

Signed for print: 30.06.2025
Paper size: A5
Volume: 38590
Number of hard copies: 70